Hindawi Publishing Corporation
Journal of Nanomaterials
Volume 2012, Article ID 129097, 7 pages
doi:10.1155/2012/129097

Research Article

Interlayer Thickness Effects on Magnetic Properties of X/FePtAg (X = FePt/Fe and Fe/FePt) Trilayers

Jai-Lin Tsai, Jian-Chiang Huang, and Hsueh-Wei Tai

Department of Materials Science and Engineering, National Chung Hsing University, Taichung 402, Taiwan

Correspondence should be addressed to Jai-Lin Tsai, tsaijl@dragon.nchu.edu.tw

Received 13 December 2011; Revised 7 February 2012; Accepted 2 March 2012

Academic Editor: Makis Angelakeris

Copyright © 2012 Jai-Lin Tsai et al. This is an open access article distributed under the Creative Commons Attribution License, which permits unrestricted use, distribution, and reproduction in any medium, provided the original work is properly cited.

A soft/hard FePt/Fe/FePtAg and Fe/FePt/FePtAg trilayers with perpendicular magnetization were prepared on a glass substrate. Inserting disordered FePt layer allowed modification of magnetic anisotropy of the Fe/FePtAg sharp interface to Fe/FePt/FePtAg stepwise interface. The out-of-plane coercivity field was modulated as a function of the FePt thickness because of the interface coupling attenuation between Fe and FePtAg. The coercivity was inversely proportional to the FePt thickness as evidenced by the pinning effect at the stepwise interface. Additionally, the out-of-plane magnetization was controlled by domain wall pinning effect. The in-plane magnetization reversal processes occurred in two steps like in exchange spring systems and attributed to the domain wall nucleation and its propagation from Fe/FePt layer into FePtAg layer.

1. Introduction

Exchange spring media and exchange coupled composite (ECC) media were introduced to reduce the write field requirement and maintain the same thermal stability and greater tolerance to easy axis distribution. ECC media and exchange spring media seem to be methods of achieving area densities of several (Tbit/in^2) [1–5]. In ECC composite media, an intermediate nonmagnetic layer modulates the exchange coupling between the hard and soft phase. In exchange spring media, a direct exchange coupling between hard and soft phase occurs where the interface between hard- and soft-magnetic materials can be ideal or graded [6, 7]. Theoretically, the coercivity field is proportional to the gradient of the densities of domain wall energy [8–11]. In graded media, the switching field can be tuned and thus enhance the exchange coupling between the hard- and soft-magnetic layer. In experimental studies, the exchange-spring soft/hard bilayer has been discussed extensively in Fe/L1$_0$ FePt bilayer systems [12–16].

This work discusses, first, the Fe magnetic interlayer thickness effects on magnetic properties of (disordered FePt)/Fe/(ordered FePtAg) trilayer. Although, the addition of a ferromagnetic intermediate layer in not suitable to tailor the coupling efficiency of an exchange-coupled bilayer, this study focuses on the effect of an additional soft magnetic layer and its effect on perpendicular magnetic anisotropy features. The interface effects are studied with the variations of in-plane and out-of-plane magnetic hysteresis loops. Second this work addresses the disordered FePt thickness effects on the magnetic properties of Fe/FePt/FePtAg trilayer. The variation of the out-of-plane coercivity was fitted by a model considering domain wall pinning and nucleation. The shape of in-plane demagnetization curves is varying with FePt thickness and correlated with inverse domain nucleation and corresponding domain wall propagation.

2. Experimental Procedures

The FePt(2 nm)/Fe(t)/FePtAg(10 nm) (t = 0, 0.5, 1, 2, 3, 5 nm) and Fe(2 nm)/FePt(t nm)/(FePtAg)(10 nm) (t = $0, 1, 3, 5, 7$ nm) trilayers were fabricated with DC (direct current) magnetron sputtering. The base pressure of the sputtering system was 2×10^{-8} Torr and the working pressure was 1.5×10^{-3} Torr under high purity argon gas. The FePt alloy target and Ag element target were used and the Ag(1 nm)/FePt(10 nm) bilayer was deposited on a glass substrate. The film chemical composition was $Fe_{48}Pt_{52}$ measured by energy dispersive spectroscopy (EDS). After

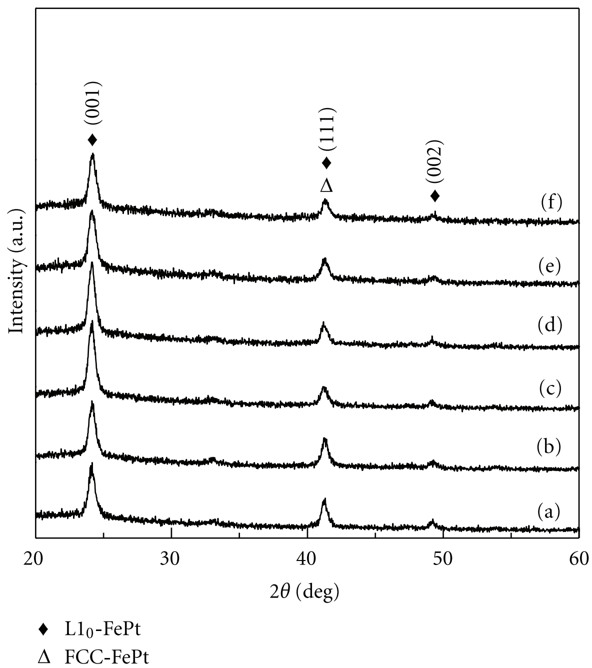

Figure 1: GID patterns of (a) FePt/FePtAg film, FePt/Fe(t)/(FePtAg) film, (b) $t = 0.5$ nm, (c) $t = 1$ nm, (d) $t = 2$ nm, (e) $t = 3$ nm, (f) $t = 5$ nm.

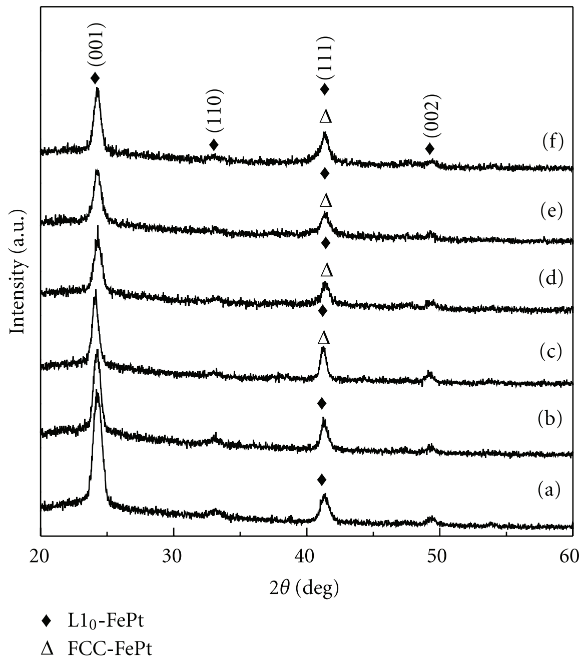

Figure 2: GID patterns of (a) Fe/(FePtAg) film, Fe/FePt(t nm)/(FePtAg) film, (b) $t = 1$ nm, (c) $t = 3$ nm, (d) $t = 5$ nm, (e) $t = 7$ nm.

deposition, the films were annealed by a rapid thermal process (RTP) at 800°C for 3 minutes and formed the FePtAg alloy film. There are two types of soft magnetic structures fabricated following two different procedures. Procedure I : Fe layer with different thicknesses from 0.5 nm to 5 nm was deposited on $L1_0$FePtAg at room temperature and capped with 2 nm of a disordered FePt layer. Finally, the FePt/Fe/FePtAg sandwich layer structure was formed. Procedure II: FePt layer was deposited on $L1_0$FePtAg layer and finally Fe layer with thickness of 2 nm was deposited on disordered FePt (t nm) layer at room temperature. The crystal structure of the samples was identified using grazing incident X-ray diffraction (GID) with Cu K_α radiation and a standard X-ray diffraction (XRD) technique (BRUKER, D8 Discover). Magnetic hysteresis loops were measured at room temperature using a vibration sample magnetometer (VSM, Lakeshore 7400) with a maximum magnetic field of 2 Tesla. The film microstructure was observed using transmission electron microscopy (TEM, Philips Tecnai F30).

3. Results and Discussion

From standard XRD pattern in previous work, the (001) superlattice diffraction peak and the (002) fundamental reflection of the $L1_0$ FePt are clearly observed in FePtAg film [17, 18]. The XRD profiles suggest that the $L1_0$ FePt crystal has a [001] texture. The ordering parameter, S can be estimated from $0.492[I(001)/I(002)]^{1/2}$, $\{[(\mathrm{I}(001)/\mathrm{I}(002)\ ]_{obs}/[\mathrm{I}(001)/\mathrm{I}002]_{cal}\}^{1/2}$ or is proportional to the ratio I(001)/I(002) [19]. The GID was used to tailor the surface structure variation of Fe/(disordered FePt) or (disordered FePt)/Fe layer. Figure 1 show GID patterns of FePt/Fe(t)/(FePtAg) ($t = 0, 0.5, 1, 2, 3, 5$ nm) films. In Figure 1(a), the FePt/FePtAg bilayer was preferred oriented at [001] direction and the relative intensity of (111) peak was low. Without the intermediate Fe layer, the interface anisotropy variation between FePt and FePtAg layer was expected to be sharp. In Figures 1(b)–1(f), the Fe layer with thickness 0.5, 1, 2, 3, or 5 nm was inserted between FePt/FePtAg bilayer. The relative intensity of diffraction peaks were almost not changed when the Fe layer was inserted. The FePt/Fe/FePtAg trilayers have (001) texture and the (111) diffraction peaks were the summation of disordered FePt and ordered FePtAg layers. Figure 2 show GID patterns of Fe(2 nm)/FePt(t nm)/(FePtAg)(10 nm) (t = 0, 1, 3, 5, 7 nm) films. In Figures 2(a)-2(b), the FePtAg single layer and Fe/FePtAg bilayer was preferred oriented at [001] direction and the relative intensity of (111) peak was low. Without disordered FePt intermediate layer, it is supposed that the interface anisotropy between Fe and FePtAg layer was sharp. In Figures 2(c)–2(f), the FePt layer with thickness of 1, 3, 5 or 7 nm was inserted between Fe/FePtAg bilayer. When the thickness of disordered FePt layer increased to 3, 5, 7 nm, the (111) diffraction peak was become rough and the full width of half maximum (FWHM) of (111) peak was increased. The disordered FePt phase existed and was proved in the variation of (111) peak. The interface anisotropy was stepwise from ordered FePtAg to disordered FePt and Fe layer. To prove the layer structure of films, the cross-section TEM images of Fe/FePtAg bilayer and Fe/FePt(3, 5 nm)/FePtAg trilayers were shown in Figure 3. With increased FePt thickness, the interface between Fe/FePt bilayer became rough but the smooth interface between FePt/FePtAg was maintained as shown in Figures 3(b)-3(c).

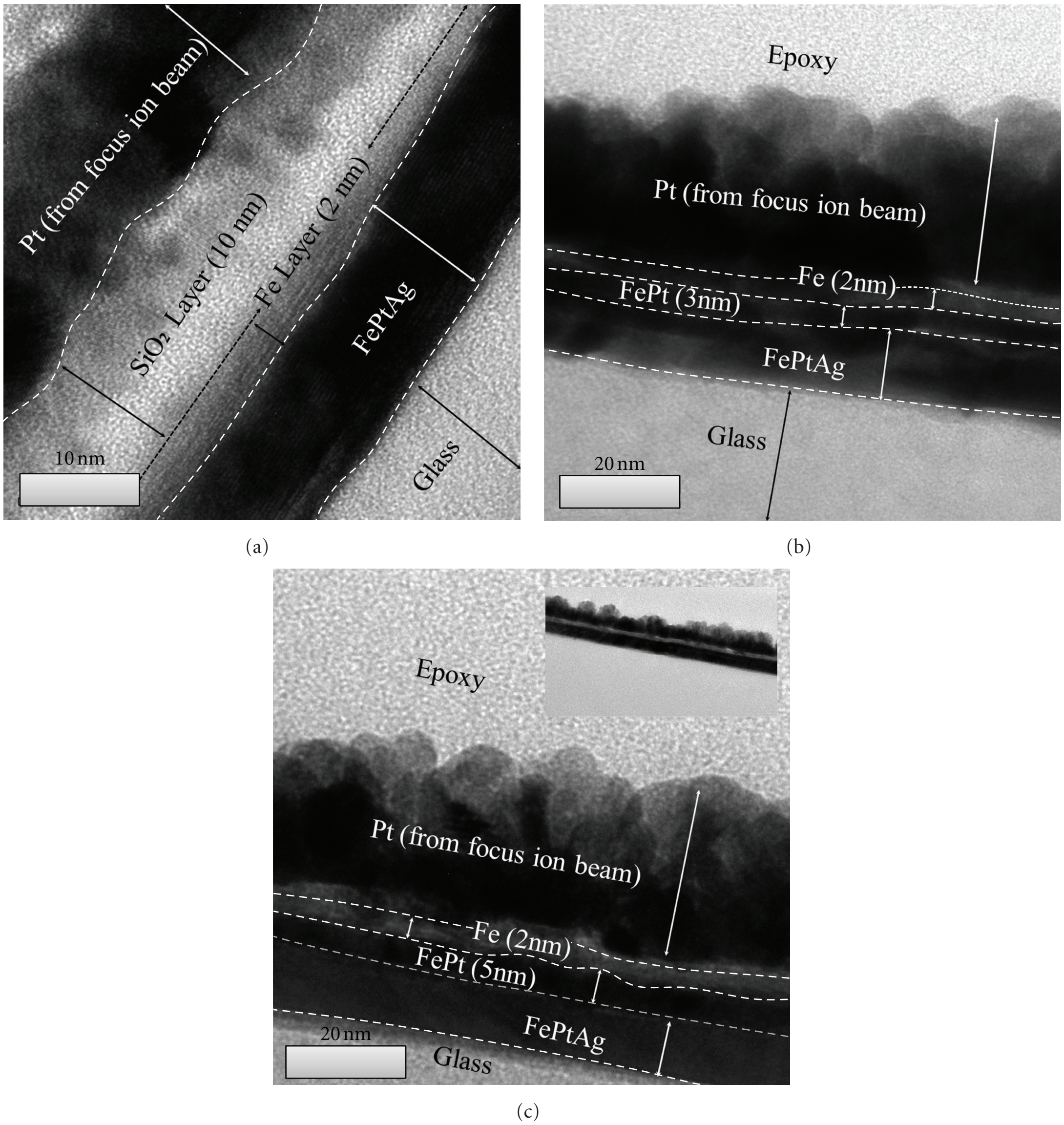

(a) (b) (c)

Figure 3: Cross-section TEM images of (a) Fe/FePtAg bilayer, (b) Fe/FePt(3 nm)/FePtAg trilayer, and (c) Fe/FePt(5 nm)/FePtAg trilayer.

From morphology, the reversed domain wall may originate from the rough interface between soft Fe/FePt. Based on the different magnetocrystalline anisotropy in Fe, FePt, and FePtAg individual layer, the magnetization was reversed stepwise from soft- to hard-magnetic layer. The coercivity was influenced more in Fe/FePt thickness and less in interface morphology.

Figure 4 show the in-plane and out-of-plane magnetic hysteresis loops of FePt/Fe/FePtAg films measured at room temperature. The in-plane and out-of-plane magnetization of glass substrate was linear with negative slope and the diamagnetic effect in FePt/glass films was computationally subtracted. In Figure 4(a), the FePt/FePtAg bilayer shows perpendicular magnetization and the out-of-plane H_c is 10.5 kOe. The disordered FePt layer with thickness of 2 nm contributed both to magnetization, in-plane and out-of-plane coercivity in FePt/FePtAg bilayer. The amount of soft-magnetic phase (FePt/Fe) increased with Fe layer thickness. The in-plane and out-of-plane coercivities decreased with amount of soft magnetic phase (FePt/Fe) or Fe layer thickness. In Figure 4(b), the Fe layer with thickness of 0.5 nm was inserted and the magnetic properties were similar to Figure 4(a). Figure 4(c) shows magnetic hysteresis loops of FePt/Fe(1 nm)/FePtAg film. For a soft magnetic Fe layer with 1 nm thickness, the out-of-plane H_c is 11.1 kOe and in-plane H_c is 3.2 kOe. The in-plane hysteresis loop is near linear and the out-of-plane hysteresis shows high perpendicular magnetization but not better than coupling of Fe/FePt bilayer in previous work [15]. The FePt/Fe/FePtAg trilayer was coupled with rigid magnetization in remanence (M_r). The remanence ratio measured at 2T is 0.72 high enough but relatively smaller than 0.98 presented in previous work on bilayer [15].

In Figures 4(d)–4(f), the FePt/Fe(2, 3, 5 nm)/FePtAg film maintains perpendicular magnetization but in-plane hysteresis also appears. The slight shoulders were measured

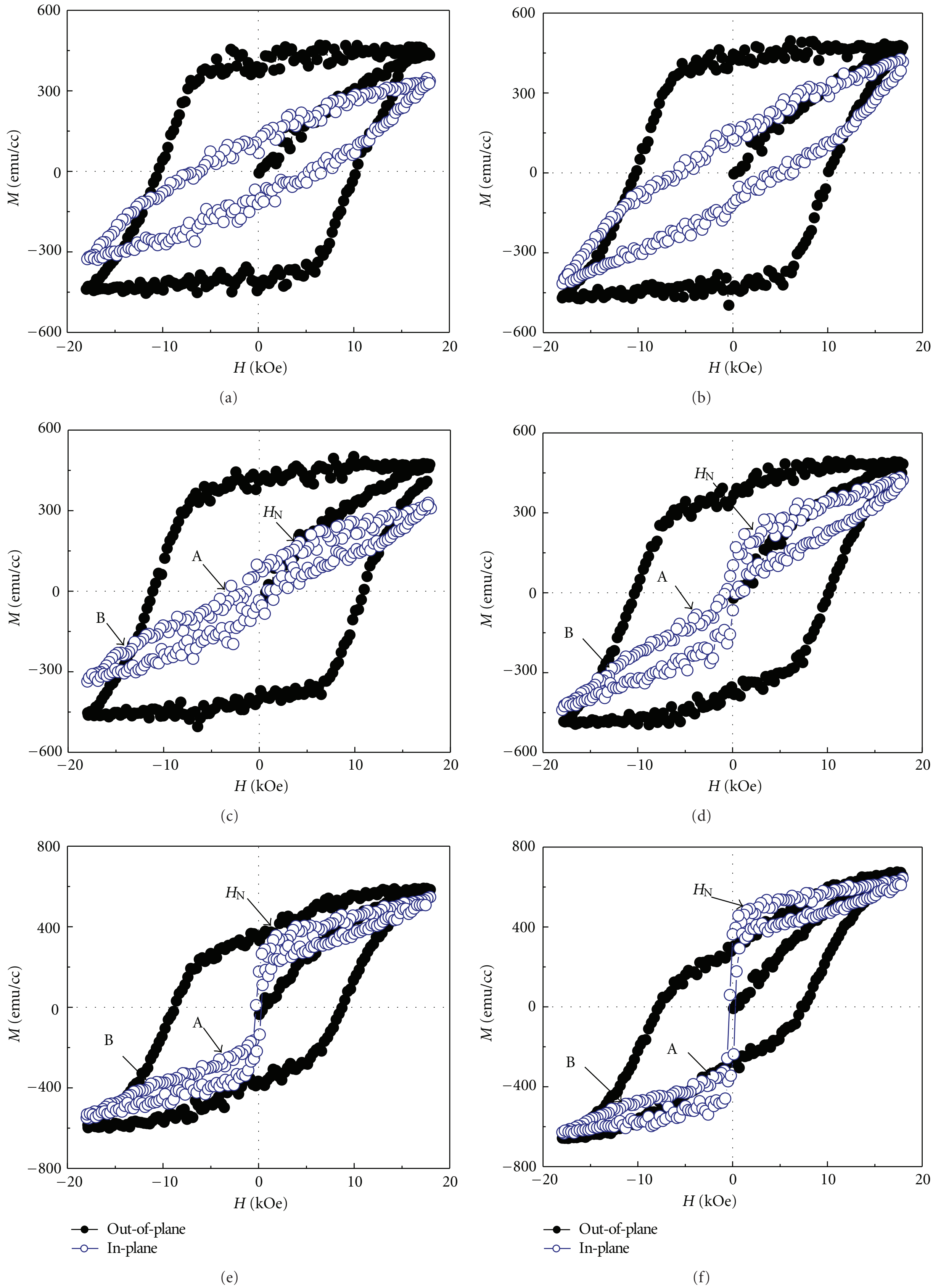

FIGURE 4: In-plane and out-of-plane magnetic hysteresis loops of (a) FePt/FePtAg film, FePt/Fe(t)/(FePtAg) film, (b) $t = 0.5$ nm, (c) $t = 1$ nm, (d) $t = 2$ nm, (e) $t = 3$ nm, (f) $t = 5$ nm.

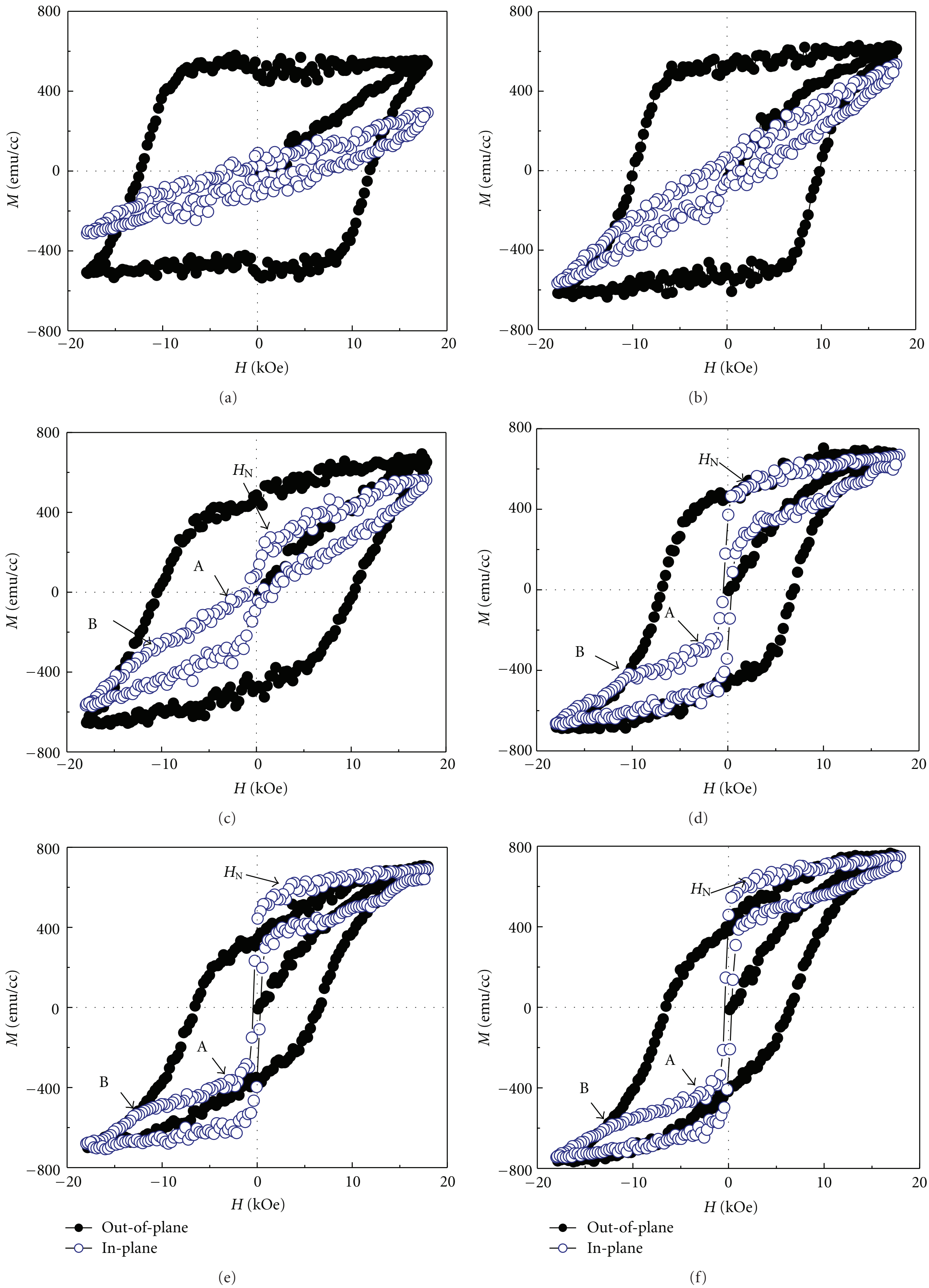

FIGURE 5: In-plane and out-of-plane magnetic hysteresis loops of (a) FePtAg film, (b) Fe(2 nm)/FePtAg film, and Fe/FePt(t)/(FePtAg) trilayer, (c) t = 1 nm, (d) t = 3 nm, (e) t = 5 nm, (f) t = 7 nm.

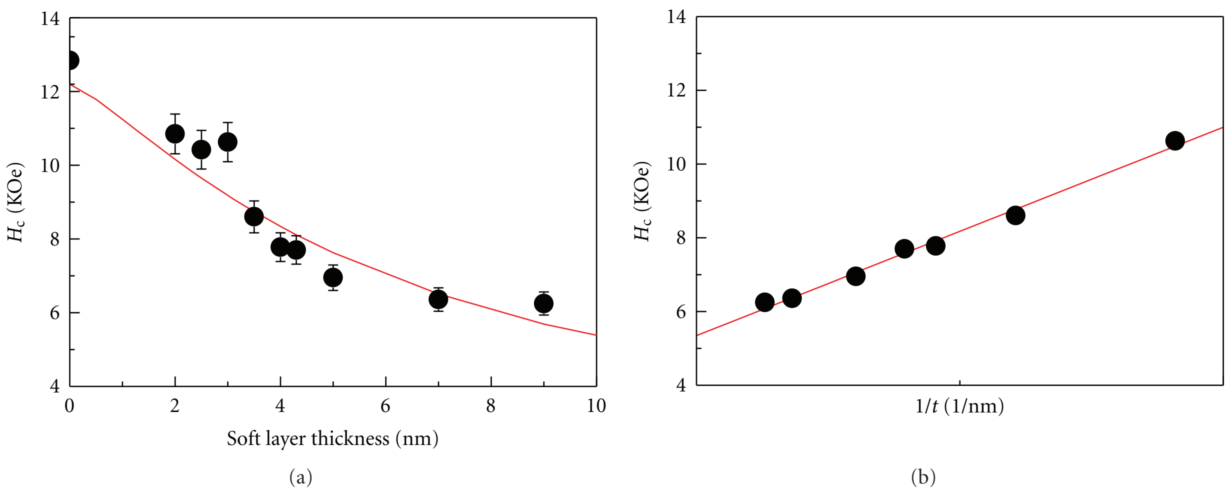

FIGURE 6: The out-of-plane H_c, as a function of (a) Fe/FePt thickness, (b) $1/t$ (t: thickness of disordered FePt layer).

in the M_r of out-of-plane hysteresis loops. The nucleation field (H_N), the switching fields of soft magnetic FePt/Fe layer (H_A) and hard magnetic FePtAg layer (H_B), and the magnetization change (ΔM) from H_N to H_A be marked in Figures 4(c)–4(f). The H_A and H_B mean the applied field of point A and B in Figures 4(c)–4(f). In the in-plane hysteresis loops, the magnetization reversal process seems to change to two-step reversal processes. The reversal domain wall was first nucleated at nucleation field (H_N) in soft-magnetic FePt/Fe layer and the magnetization of FePt/Fe was reversed at H_A field. Then the domain wall was propagated from the FePt/Fe layer into the FePtAg layer. The magnetization of FePtAg layer was switched at H_B field. Moreover, the values of positive H_N and ΔM were increased with inserted Fe layer thickness due to the amount of soft magnetic phase FePt/Fe(t). The Fe layer was used to test the maximum amount of soft phase FePt/Fe. Above the limited Fe layer thickness, the two steps magnetization reversal was appeared in in-plane loop and the shoulder or remanence declination was evidenced in out-of-plane loop.

Figure 5 shows in-plane and out-of-plane magnetic hysteresis loops of FePtAg film and Fe/FePt(t nm)/(FePtAg) trilayer measured at room temperature. In Figure 5(a), the FePtAg film shows perpendicular magnetization and the out-of-plane H_c is 12.8 kOe. Figure 5(b) shows magnetic hysteresis loops of Fe(2 nm)/(FePtAg) bilayer. The out-of-plane H_c is 11.7 kOe and in-plane H_c is 0.12 kOe. Without disordered FePt layer, the in-plane loop is linear shape due to less amount of soft magnetic phase. Both in-plane and out-of-plane coercivity deceased with the thickness of disordered FePt layer. The in in-plane hysteresis loops deviated from a linear shape, indicating that the amount of soft-magnetic phase Fe/FePt(t) increased and the magnetization turns easily to the in-plane direction under an applied field. In Figures 5(c)–5(f), the interface coupling was changed to exchange-spring like behavior in the in-plane hysteresis loops. The magnetization reversal process was changed from a single switching field to two-step reversal processes. The reversed domain wall appeared in positive nucleation field (H_N) and the magnetization of soft Fe/FePt layer was switched at H_A field. The varied magnetization in-between H_N and H_A increased with the thickness disordered FePt. Finally, the domain walls were propagated from the Fe/FePt layer into the FePtAg layer. The magnetization of hard FePtAg layer was reversed at H_B field.

Figure 6(a) shows the soft magnetic layer (Fe/(disordered FePt)) thickness effect on the out-of-plane coercivity field of Fe/FePt/FePtAg composite films. The coercivity is reduced from 12.8 kOe to 6.5 kOe for FePtAg film and Fe/FePt(7 nm)/FePtAg composite film, respectively. The coercivity field is reduced drastically by a factor of 2 when the total thickness of Fe(2 nm)/FePt(7 nm) bilayer reaches 9 nm. This behavior is a typical two-phase system in which the soft layer thickness exceeds the Bloch wall domain wall width of hard phase [3, 9]. According to the analytical result with modified coefficients, $H_c(\text{Fe/FePt}) = [10.5/(t_{\text{soft}}^{1.27} + 8.6) + 0.17]$, the measured coercivities were fitted approximately by a $1/t_{\text{soft}}^{1.27}$ relation [6, 7]. The measured coercivities were fitted by a $1/d_{\text{soft}}^{1.27}$ relation. In Figure 6(b), the out-of-plane coercivity of Fe/FePt/FePtAg film is plotted against ($1/t_{\text{FePt}}$). The linear relationship is optimally obtained in H_c versus ($1/t_{\text{FePt}}$) curve which was due to pinning at stepwise interface created by disordered FePt layer. The slope of line is given by 4.34. The value of the saturation magnetization (M_s) and the exchange stiffness constant (A) were assumed to be 1600 emu/cm^3 and 10^{-6} erg/cm^3. The maximum hard phase magnetocrystalline anisotropy energy (K_u) is 2.7×106 erg/cm^3 that derived from slope in Figure 6(b) with equation $(\text{AK})^{1/2}/(2M_s)$ [4, 9]. Nucleation controlled magnetization reversal is expected in $1/t_s^2$ law and the magnetization reversal of Fe/FePt/FePtAg film is suppose to follow $1/t_{\text{FePt}}$ law evidenced in Figure 6.

The results obtained previously by Kronmüller and Goll [8] for the thickness dependence of the nucleation fields are $1/d$ and $1/d^2$. Fullerton et al. [12] clearly show that the coercivity field decreased strongly by a factor of 3 or 4 for soft-magnetic layer thickness up to 4 nm. Experimental results of the thickness dependence of the coercivity field of composite films have been determined by Goll and Breitling [6, 7] for the ledge-type Fe/FePt system indicating a $d^{-1.38}$ law for the thickness dependence.

4. Conclusions

In conclusion, FePt/Fe/FePtAg and Fe/FePt/FePtAg films with perpendicular magnetization were prepared on glass substrate. The Fe interlayer thickness increased the amount of soft magnetic phase in (disordered FePt)/Fe/($L1_0$ FePt-Ag) film. When the thickness of Fe layer is kept under 1 nm, the perpendicular anisotropy was maintained. In Fe/FePt/FePtAg trilayer, the disordered FePt layer was inserted as pinning layer and actually reduced the coupling between Fe and FePtAg. The coercivity field was modulated and found inversely proportional to the thickness of FePt layer. The in-plane magnetization reversal process of exchange spring like Fe/FePt/FePtAg film was interpreted by domain wall-assisted depinning and motion around the hard/soft interface. Finally, the inserted disordered FePt or Fe layer only increased the amount of soft magnetic phase and acted as an attenuating mechanism of the perpendicular magnetization of bilayer revealing thickness-dependent variations of magnetic properties.

Acknowledgments

The authors would like to thank the NSC for financial support under Grant no. NSC 100-2221-E-005-044-MY2. They also thank Dr. Y. H. Pai and the Center of Nanoscience and Nanotechnology in NCHU for the TEM investigation.

References

[1] R. H. Victora and X. Shen, "Composite media for perpendicular magnetic recording," *IEEE Transactions on Magnetics*, vol. 41, no. 2, pp. 537–542, 2005.

[2] J. P. Wang, W. K. Shen, J. M. Bai, R. H. Victora, J. H. Judy, and W. L. Song, "Composite media (dynamic tilted media) for magnetic recording," *Applied Physics Letters*, vol. 86, Article ID 142504, 3 pages, 2005.

[3] A. Y. Dobin and H. J. Richter, "Domain wall assisted magnetic recording," *Applied Physics Letters*, vol. 89, no. 6, Article ID 062512, 2006.

[4] D. Suess, T. Schrefl, S. Fähler et al., "Exchange spring media for perpendicular recording," *Applied Physics Letters*, vol. 87, no. 1, Article ID 012504, 3 pages, 2005.

[5] D. Weller, A. Moser, L. Folks et al., "High ku materials approach to 100 gbits/in2," *IEEE Transactions on Magnetics*, vol. 36, no. 1, pp. 10–15, 2000.

[6] D. Goll, A. Breitling, L. Gu, P. A. Van Aken, and W. Sigle, "Experimental realization of graded $L1_0$ -FePt/Fe composite media with perpendicular magnetization," *Journal of Applied Physics*, vol. 104, no. 8, Article ID 083903, 2008.

[7] D. Goll and R. Breitling, "Coercivity of ledge-type $L1_0$-FePt/Fe nanocomposites with perpendicular magnetization," *Applied Physics Letters*, vol. 94, Article ID 052502, 3 pages, 2009.

[8] H. Kronmüller and D. Goll, "Pinning of domain walls in composite particles," *Physica B*, vol. 403, no. 2-3, pp. 237–241, 2008.

[9] D. Suess, "Multilayer exchange spring media for magnetic recording," *Applied Physics Letters*, vol. 89, no. 18, Article ID 113105, 2006.

[10] A. Goncharov, T. Schrefl, G. Hrkac et al., "Recording simulations on graded media for area densities of up to 1 Tbit in.2," *Applied Physics Letters*, vol. 91, no. 22, Article ID 222502, 2007.

[11] R. Skomski, T. A. George, and D. J. Sellmyer, "Nucleation and wall motion in graded media," *Journal of Applied Physics*, vol. 103, no. 7, Article ID 07F531, 2008.

[12] E. E. Fullerton, J. S. Jiang, M. Grimsditch, C. H. Sowers, and S. D. Bader, "Exchange-spring behavior in epitaxial hard/soft magnetic bilayers," *Physical Review B*, vol. 58, no. 18, pp. 12193–12200, 1998.

[13] J. P. Wang, W. Shen, and S. Y. Hong, "Fabrication and characterization of exchange coupled composite media," *IEEE Transactions on Magnetics*, vol. 43, no. 2, pp. 682–686, 2007.

[14] F. Casoli, F. Albertini, L. Nasi et al., "Strong coercivity reduction in perpendicular FePtFe bilayers due to hard/soft coupling," *Applied Physics Letters*, vol. 92, no. 14, Article ID 142506, 2008.

[15] J. L. Tsai, H. T. Tzeng, and G. B. Lin, "Magnetization reversal process in Fe/FePt films," *Applied Physics Letters*, vol. 96, Article ID 032505, 3 pages, 2010.

[16] J. L. Tsai, H. T. Tzeng, and B. F. Liu, "Magnetic properties and microstructure of graded Fe/FePt films," *Journal of Applied Physics*, vol. 107, no. 11, Article ID 113923, 2010.

[17] J. L. Tsai, H. W. Tai, J. C. Huang, C. S. Lin, and L. H. Chen, "Magnetic properties and microstructure of exchange coupled Fe/(FePt-Ag_2Se) particulate films ," *IEEE Transactions on Magnetics*, vol. 47, no. 10, pp. 3625–3628, 2011.

[18] J. L. Tsai, J. C. Huang, and H. W. Tai, "Magnetic properties and microstructure of perpendicular FePt(B-Ag) granular films," *Journal of Applied Physics*, vol. 111, Article ID 07A709, 3 pages, 2012.

[19] L. Zhang, Y. K. Takahashi, A. Perumal, and K. Hono, "$L1_0$-ordered high coercivity (FePt)AgC granular thin films for perpendicular recording," *Journal of Magnetism and Magnetic Materials*, vol. 322, no. 18, pp. 2658–2664, 2010.

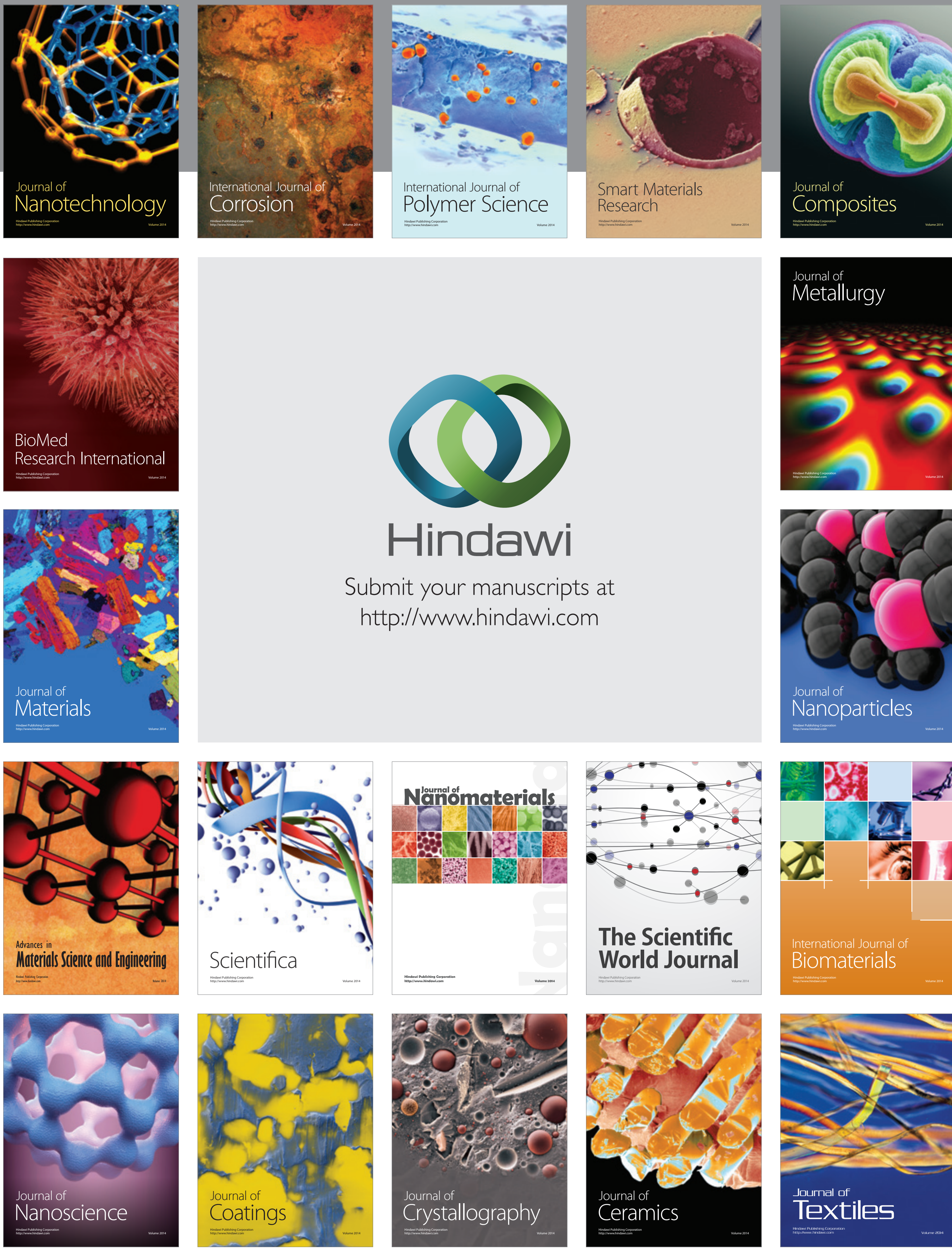
Journal of Nanotechnology
International Journal of Corrosion
International Journal of Polymer Science
Smart Materials Research
Journal of Composites
BioMed Research International
Hindawi
Submit your manuscripts at
http://www.hindawi.com
Journal of Metallurgy
Journal of Materials
Journal of Nanoparticles
Advances in Materials Science and Engineering
Scientifica
Journal of Nanomaterials
The Scientific World Journal
International Journal of Biomaterials
Journal of Nanoscience
Journal of Coatings
Journal of Crystallography
Journal of Ceramics
Journal of Textiles